General Lectures

AMAS COURSE ON RELIABILITY-BASED DESIGN AND OPTIMISATION
RBO'03 – (PP.9–41) – WARSAW, SEPTEMBER 15-18, 2003

Probability of collapse of monumental buildings under horizontal loads

G. AUGUSTI and M. CIAMPOLI

Department of Structural and Geotechnical Engineering
Università di Roma "La Sapienza"
Via Eudossiana 18, I-00184 ROMA, Italy
giuliano.augusti@uniroma1.it

In recent years, the assessment of the seismic reliability of monumental buildings has been the object of several studies: in order to take into account the large uncertainties in the loads and in the material and structural properties, in most studies the seismic action has been mimicked by quasi-static horizontal forces of magnitude depending on the intensity of the considered earthquake. In particular, it has been shown that the probabilities of damage and collapse and their distributions can be obtained by looking at a monumental building as an assemblage of macroelements of known static and collapse behaviour, and considering the relevant mechanisms: in this way, the so called *kinematic approach* to limit analysis is followed, and rigourously only lower bounds to the probability of collapse are obtained. In order to obtain also upper (i.e. "safe") bounds to the probability of collapse under a given load, the static theorem of probabilistic limit analysis must be used. In this lecture, the two theorems are presented, and the procedure of seismic reliability assessment exemplified on two churches damaged in the 1976 earthquake of Friuli (North-East Italy): upper and lower bounds to the probability of collapse of each macroelement and of the whole church are obtained as a function of the applied horizontal load, i.e. of the earthquake intensity.

1. Introduction: the "macroelement" approach

The static and kinematic theorems of "probabilistic limit analysis", first formulated in 1972 by Augusti and Baratta, yield bounds to the probability of plastic collapse under given loads of structures with random strength properties.

The static theorem states that the probability of not finding an admissible stress field in equilibrium with given loads is not smaller than the actual probability of collapse, provided the usual assumptions of rigid-plastic limit analysis hold.

Conversely, the kinematic theorem states that the actual probability of collapse is not smaller than the probability that the work done by given applied loads for an arbitrary collapse mechanism exceeds the corresponding dissipated internal power.

Thus, for a given structure, whose mechanical and geometrical properties have known probabilistic characteristics, subject to a set of static loads defined to within a factor α (i.e. in the form $\mathbf{W}_0 + \alpha\mathbf{W}$), the cumulative probability distribution curve of the actual collapse load factor $\alpha = \alpha_C$ is bounded between the analogous curves for the static and kinematic collapse load factors.

In the present lecture the static and kinematic approaches are applied, to assess and bound on both sides the probability of collapse of monumental buildings, and specifically of historic masonry churches, under static horizontal loads of arbitrary direction, and proportional to the structural masses (thus mimicking seismic loads).

The relevant uncertain quantities (including the direction of the horizontal load) are assumed to satisfy discrete probability distributions.

For the structural analysis and assessment of the considered buildings, we shall follow the "macroelement" approach, first formulated in 1994 [Doglioni *et al.*, 1994]. A "macroelement" is defined as "a recognisable and complete part of the building, with a clear and unitary behaviour from the viewpoint of seismic response"; then, each building under examination is considered as the assemblage of macroelements (e.g. facade; nave walls; arches; chapels). Several examples of each macroelement can be found among buildings of the same geographical area. In this way, not only the ultimate behaviour of the buildings is well schematised, but the contradiction between the need of probabilistic assessment of vulnerability and reliability and the uniqueness of each monumental building can be overcome: probabilistic predictions of the response become possible, even for "unique" structures like historic churches.

The resistance and collapse conditions of each macroelement are obtained from the study of its seismic response; the assumption of an appropriate "logical diagram" allows to derive the collapse condition of the whole church.

2. Formulation of the limit analysis problem

2.1. Assessment of seismic strength in limit analysis

In "classical" limit analysis it is usually assumed that the structure under examination is subject to a set of static loads defined to within a factor α, i.e. in the form

$$\mathbf{W}_0 + \alpha\mathbf{W}, \tag{2.1}$$

where $\mathbf{W}_0$ is a fixed vector (permanent loads) and $\mathbf{W}$ a reference vector. The value of α that corresponds to the collapse of the structure (or a part of it) is defined *collapse load factor*, and indicated in the following by α_C.

We shall also indicate by α_ψ a *"statically admissible" load factor*, i.e. a coefficient such that the loads $\mathbf{W}_0+\alpha_\psi\mathbf{W}$ can be equilibrated by a stress field that does not violate the strength condition in any point of the structure, and by α_γ a *"kinematically sufficient" load factor*, i.e. a coefficient such that there exists at least one kinematically sufficient mechanism, in turn defined as a mechanism for which the power of the work done by the loads $\mathbf{W}_0 + \alpha_\gamma\mathbf{W}$ is not smaller than the dissipated internal power.

Well known theorems (valid, in full rigour, only for elastic-plastic structural behaviour) prove that, for any given structure of known geometry and material properties,

$$\alpha_\psi \leqslant \alpha_C \leqslant \alpha_\gamma. \tag{2.2}$$

Thus, the determination of *statically admissible* and *kinematically sufficient* load factors allows to bound the true value of the *collapse load factor*.

Much research effort has been spent over the last few decades on methodologies to find close bounds, or alternatively to minimize the *kinematically sufficient* load factor: in fact, the *kinematic approach* has been generally preferred to the *static approach* because simpler to use and usually leading to better approximations for comparable amounts of computing effort. This has however often lead to forgetting that in this way results on the "unsafe" side are obtained if not all possible collapse mechanisms are taken into consideration: therefore, the validity of the static approach should be reconsidered, now that much more powerful computing hard- and software are available than even a few years ago.

In most cases, the seismic strength of a masonry structure under an earthquake of any given intensity can be studied with reference to quasi-static loads defined in accordance with Eq. (2.1). $\mathbf{W}_0$ are vertical loads, usually identified with the weights of the building masses (and possibly other quasi-permanent imposed loads), while the seismic loads $\alpha\mathbf{W}$ are considered as static horizontal loads: the horizontal load vector $\mathbf{W}$ is assumed equal to $\mathbf{W}_0$ (or part of it), and the proportionality coefficient α is taken equal to the ratio $\alpha = a_g/g$ between a representative value (typically, the *peak*) of the (horizontal) ground acceleration a_g and the acceleration of gravity g; α is thus a measure of the intensity of the earthquake.

In the following, the *collapse factor* α_C of the seismic load will be called also *seismic strength coefficient* (or more simply *seismic coefficient*) of the structure; it can be assumed as a measure of its seismic resistance. Note that in Sec. 3.1.1, a "*mechanism seismic coefficient*" is defined.

For the seismic strength assessment the structures considered in this paper, it is convenient to decompose first the building into *macroelements*, that is large elements (facade, lateral walls, arches, bell tower, etc.), which – according to the experience of past earthquakes – respond as single units to seismic action, and for which the main features of the seismic response are at least approximately known. It is then possible to carry out the limit analysis for each macroelement, i.e. to investigate collapse mechanisms and equilibrated stress fields.

Moreover, in application to seismic problems, it is important to keep in mind (although often neglected in the formulation of the limit analysis problems in seismic engineering) that the direction (and sign) of the horizontal loads $\alpha\mathbf{W}$ is not predetermined, but random: however, inequalities (2.2) hold for any given direction θ, namely

$$\alpha_{\psi}(\theta) \leqslant \alpha_{\mathrm{C}}(\theta) \leqslant \alpha_{\gamma}(\theta). \tag{2.3}$$

In principle, statically admissible stress fields and kinematically sufficient mechanisms should be investigated over the whole range of θ. However, in order to find bounds on $\alpha_{\mathrm{C}}(\theta)$ it is necessary to determine only the values of $\alpha_{\psi}(\theta)$ and $\alpha_{\gamma}(\theta)$ in two orthogonal directions (for example, x and y in Fig. 1) and remember that, as well known from the general theory of plasticity, the limit condition $\alpha_{\mathrm{C}}(\theta)$ is a closed convex curve in the $x-y$ plane: thence, it will be bounded between the rhomb defined by $\alpha_{\psi}(\pm x)$, $\alpha_{\psi}(\pm y)$ and the rectangle defined by $\alpha_{\gamma}(\pm x)$, $\alpha_{\gamma}(\pm y)$, i.e. included in the shaded

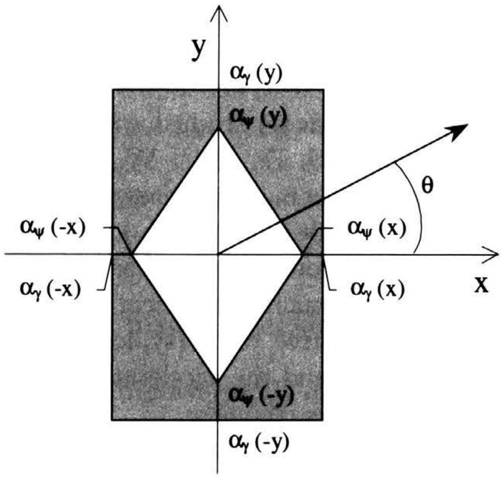

FIGURE 1. Bounds to the limit domain $\alpha_{\mathrm{C}}(\theta)$ as a function of the force direction.

area in Fig. 1. Thus, in the quadrant $x \geqslant 0$; $y \geqslant 0$, values of the *statically admissible* and *kinematically sufficient* load factors are respectively given by

$$\alpha_{\psi}(\theta) = \frac{\alpha_{\psi}(x) \cdot \alpha_{\psi}(y)}{\alpha_{\psi}(x) \cdot \cos\theta + \alpha_{\psi}(y) \sin\theta}, \tag{2.4}$$

$$\alpha_{\gamma}(\theta) = \min\left[\frac{\alpha_{\gamma}(x)}{\cos\theta}, \frac{\alpha_{\gamma}(y)}{\sin\theta}\right]. \tag{2.5}$$

Analogous formulas hold in the other quadrants.

In practice, such bounds are usually sufficient. Note that in Fig. 1 and in Eqs. (2.4) and (2.5), symmetric strength properties have been assumed, that is:

$$\begin{aligned} \alpha_{\psi}(x) &= \alpha_{\psi}(-x), \quad \alpha_{\psi}(y) = \alpha_{\psi}(-y), \\ \alpha_{\gamma}(x) &= \alpha_{\gamma}(-x), \quad \alpha_{\gamma}(y) = \alpha_{\gamma}(-y). \end{aligned} \tag{2.6}$$

However, Fig. 1 and Eqs. (2.4) and (2.5) can be easily generalized if equalities (2.6) do not hold. In applications, the same directions x and y can be taken for all macroelements, or different appropriate directions can be chosen for each macroelement (e.g., for a wall element, the in-plane and the out-of-plane directions).

2.2. Static and kinematic theorems of probabilistic limit analysis and their application to the assessment of seismic strength

Probabilistic limit analysis can be defined as the limit analysis of structures with random strength properties, while usually possible uncertainties in the loads are treated separately. It is based on the following generalization of inequalities (2.2).

A number of possible equilibrated stress fields and collapse mechanisms are first individuated and chosen. Then, for any value of α, three events can be defined, namely:

- *collapse* of the structure (or part of it);
- E_{stat}: among the investigated stress fields, none is statically admissible (i.e. is in equilibrium with the loads $\mathbf{W}_0 + \alpha\mathbf{W}$ and does not violate the strength condition in any point of the structure);
- E_{cin}: among the investigated mechanisms, at least one is kinematically sufficient.

Since E_{cin} implies structural collapse, which in turn implies E_{stat}, it is immediate that the probabilities of the three events are related by

$$P[E_{\text{stat}}] \geqslant P[\textit{collapse}] = P_{\text{f}} \geqslant P[E_{\text{cin}}]. \tag{2.7}$$

Hence, the cumulative probability distribution curve $P(\alpha_C)$ of the actual collapse load factor α_C is bounded between the analogous curves of the static and kinematic collapse load factors:

$$P(\alpha_\psi) \geqslant P(\alpha_C) \geqslant P(\alpha_\gamma). \tag{2.8}$$

Values of α_ψ and α_γ can thus be calculated from the chosen equilibrated stress fields and collapse mechanisms.

As in "classical" limit analysis, the kinematic approach, although yielding a result on the "unsafe" side (a collapse probability smaller than actual is obtained if not all possible collapse mechanisms are taken into consideration), has been more widely used also in probabilistic limit analysis, because of its comparably greater simplicity and better approximation is usually achieved for comparable amount of computing effort. Recently however, the static theorem is being paid again an increasing attention.

If the structure under consideration is decomposed into *macroelements*, it is possible to carry out the probabilistic limit analysis for each macroelement, i.e. to investigate static collapse mechanisms and equilibrated stress fields: once the probability of collapse of each macroelement is obtained (or bounded), it is simple to derive the (bounds to the) probability of collapse of the whole church if the macroelements are related by a logical diagram.

An approach to this problem (that will be illustrated in Sec. 3 and 4) is to take into consideration several (the most likely) collapse mechanisms of each macroelement and to evaluate the values and probability distributions of the corresponding collapse factors (specifically, in the example presented, the collapse factors were assumed to be normally distributed around the nominal value); then to calculate the probabilities of activation of the considered mechanisms under a given intensity of the horizontal load and, by combining appropriately the probabilities of activation of each mechanism, the probability of collapse of each macroelement.

In this approach, the direction of the horizontal action is taken into account by investigating two sets of kinematically sufficient mechanisms, corresponding to collapse in two orthogonal planes (in most cases, in-plane and out-of-plane for the relevant macroelement).

Rigourously, according to the kinematic theorem of probabilistic limit analysis, notwithstanding the high number of mechanisms investigated, only lower (although possibly very close) bounds to the probabilities of collapse are thus obtained. As it will be seen, this approach allows to investigate also the probabilities of damage, although defined in a rather conventional way. Alternatively, the "kinematic theorem" and the "static theorem" can be used together to derive probability bounds, as in the example presented in Sec. 5.

In the development of this example, instead of attributing a continuos probability distribution to the evaluated collapse load factors, the probabilistic properties of the relevant parent quantities (material and geometrical properties, vertical loads and direction of horizontal action) are taken directly into consideration, assuming for all these quantities discrete probability distributions (i.e. probability mass functions [pmf] instead of probability density functions [pdf]); thus, the number of possible combinations of values of the random variables is finite.

In order to obtain lower bounds $P(\alpha_\gamma)$ to the actual probability of collapse $P(\alpha_C)$, the values of α_γ obtained for each combination of the relevant random variables are convoluted with their assumed probability distributions; the dependence of α_γ on the direction of the horizontal action is given by Eq. (2.5). To obtain also upper bounds $P(\alpha_\psi)$ to $P(\alpha_C)$, equilibrated stress fields must be investigated to find which ones are statically admissible for each combination of random variables: the corresponding load factors are then convoluted with the probabilities of each combination.

The randomness of the direction θ of the horizontal action is taken into account by evaluating the bounds to the conditional probability of collapse on an assumed θ, and combining them according to the assumed probability distribution of θ.

The two just summarized procedures will be illustrated with reference to two specific example of 18^{th} century churches, heavily damaged (but not destroyed) by the 1976 Friuli earthquake: *Santa Maria del Fossale* in the town of Gemona (Fig. 2) and *Santa Maria Maddalena* in the village of Flagogna (Fig. 9). The main data on both churches have been taken from [Doglioni *et al.*, 1994].

3. Estimating the vulnerability and damages of churches by the kinematic approach

As already stated, the structure is assumed to be loaded by given vertical loads $\mathbf{W}$ and quasi-static horizontal loads $\alpha\mathbf{W}$. The proportionality coefficient α a (ratio between horizontal and vertical loads) is conventionally taken equal to the ratio a_g/g between a significant (peak or effective) ground acceleration and the acceleration of gravity; the value of a_g is considered a first-approximation measure of the intensity of the earthquake to which the structure is assumed to be subjected.

To evaluate the probability of collapse, first the macroelements that define the structural organism of the building (in the example case, a church) and characterize its seismic response must be individuated. Typical macroelements of a masonry church are: facade; nave walls; "triumphal" arches between nave and presbytery and between presbytery and apse; presbytery walls; lateral chapels; apse (cf. Fig. 2).

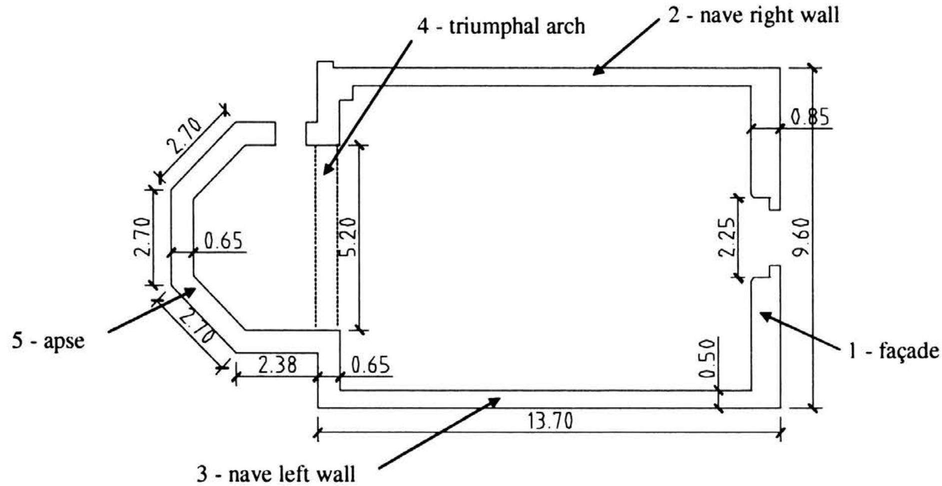

FIGURE 2. Church of Santa Maria del Fossale in the town of Gemona: plan and considered macroelements (all measures in meters).

With respect to response to seismic action, the macroelements can be classified into four main typologies, namely:

(a) wall, with or without openings in any possible arrangement, and with or without restraints along the length or at the border (e.g. facade or lateral walls of the nave or of the presbytery),
(b) arch (e.g. the element between the nave and the presbytery or between the presbytery and the apse),
(c) tower, an element that behaves as a cantilever with box cross section, with or without openings, in any possible arrangement (e.g. the bell tower),
(d) apse or lateral chapel, with curvilinear plan.

3.1. Evaluation of the vulnerability

3.1.1. For each macroelement: Once the structure has been subdivided into appropriate macroelements:

(a) the most significant collapse mechanisms (i) for each macroelement (j) are recognized,
(b) by means of the kinematic approach of limit analysis, the nominal values of the *mechanism seismic coefficient* C_{ij} (defined as the value of

the coefficient α that corresponds to the activation of the mechanism i in macroelement j), are obtained for each i and j,

(c) the probability density functions (pdf) $f_{C_{ij}}$ of the mechanism seismic coefficients C_{ij} are defined: in the presented example, each C_{ij} has been assumed to be normally distributed, with mean value $E[C_{ij}]$ equal to the value calculated in step (b), and coefficient of variation (c.o.v.) estimated on the basis of the number, the significance and the uncertainties of the parameters considered in step (b) (appropriate research might allow a better identification of shape and parameters of these distributions),

(d) for each given value of a_{g}, the probability P_{ij} of activation of the i-th mechanism for the j-th macroelement is calculated as follows:

$$P_{ij} = \mathrm{Prob}\Big[C_{ij} \leqslant \frac{a_{\mathrm{g}}}{g}\Big] = F_{C_{ij}}\Big(\frac{a_{\mathrm{g}}}{g}\Big) = \int\limits_{0}^{a_{\mathrm{g}}/g} f_{C_{ij}}(C_{ij})\, dC_{ij}, \tag{3.1}$$

where $f_{C_{ij}}$ is the pdf defined under (c) above and $F_{C_{ij}}$ denotes the corresponding cumulative distribution function (CDF);

(e) for each value of a_{g}, the collapse probability P_j of the j-th macroelement (defined as the activation of *any* mechanism) is calculated. To this end, it is assumed that the collapse mechanisms of a macroelement can be either independent [ind] or mutually exclusive [me] (the latter condition represents, for example, most relations between in-plane and out-of-plane mechanisms). The probability of combination of "ind" and "me" mechanisms among themselves is given by either of the well-known formulae respectively valid for independent and mutually exclusive events; hence, the corresponding probabilities of collapse $P_{j,\mathrm{ind}}$ and $P_{j,\mathrm{me}}$ are:

$$P_{j,\mathrm{ind}} = \sum_{i} P_{ij} - \sum_{i_1 \neq i_2} P_{i_1 j} P_{i_2 j} + \sum_{i_1 \neq i_2 \neq i_3} P_{i_1 j} P_{i_2 j} P_{i_3 j} - \ldots, \tag{3.2}$$

$$P_{j,\mathrm{me}} = \sum_{i} w_{ij} P_{ij}, \tag{3.3}$$

where w_{ij} is a weighting factor, whose value is related to the probability of activation of the i-th collapse mechanism in the j-th macroelement. Again, the present stage of research allows only rough, rule-of-the-thumb evaluations of the w_{ij} coefficients: an example is reported in Sec. 4 below (Table 4).

TABLE 1. Considered macroelement types and collapse mechanisms.

Macroelement	Collapse Mechanism
Facade	1a. Out-of-plane rotation due to the development of a horizontal cylindrical hinge at the basis of the facade, and to the detachment from orthogonal walls, 1b. Out-of-plane rotation due to the development of a horizontal cylindrical hinge corresponding to the top of the openings (entry, windows), and to the detachment from orthogonal walls, 2a. Out-of-plane rotation of the top of the facade, 2b. Out-of-plane rotation due to the development of oblique cylindrical hinges, 3a. In-plane failure due to cracks with x trend, 3b. Detachment corresponding to the middle of the facade, and translation in the plane of the facade.
Nave lateral walls	4a. Out-of-plane rotation of a wall restrained on three sides but free on the top side, 4b. Out-of-plane rotation of a wall restrained on four sides, 4c. Out-of-plane rotation of a wall restrained on the bottom side and free on the other three (4c1: cylindrical hinge at the base of the wall; 4c2: cylindrical hinge corresponding to openings, such as windows). 5. Collapse due to localized thrusts from the roof, 6. Planar sliding due to oblique (X-shaped) cracks,
Nave as a whole	7. Collapse due to transversal seismic action: cracks in the transversal arches; crushing or cracking at the base of the nave pillars, 8. Collapse due to longitudinal seismic action: cracks in the longitudinal arches; crushing or cracking at the base of the nave pillars, 9. Cracks and/or disconnection of the vault ribs,
Triumphal arch	10. Shear failure of haunches, 11a. Rotation of one haunch, 11b. Rotation of both haunches,
Apse	12a. Rotation and translation of the top with detachment along an inclined plane (often in circular and polygonal apses), 12b. Out-of-plane rotation due to the development of a horizontal cylindrical hinge at the basis of the apse end wall (usually in rectangular apses), 13a. Out-of-plane rotation due to the development of hinges corresponding to the edges, 13b. Out-of-plane rotation of vertical bends, 14. Planar sliding due to cracks with x trend,
Presbytery	4a, 4b, 4c, 5, 6, 7, 8, 9,
Transept – facade Transept – nave	1a, 1b, 2a, 2b, 3a, 3b, 4a, 4b, 4c, 5, 6, 7, 8, 9
Lateral chapels	12a, 12b, 13, 14.

(f) the probability of combination of a set of "me" mechanisms with a set of "ind" ones is given, after Eq. (3.2), by:

$$P_j = P_{j,\mathrm{me}} + P_{j,\mathrm{ind}} - P_{j,\mathrm{me}} P_{j,\mathrm{ind}}. \tag{3.4}$$

Repeated application of Eqs. (3.2), (3.3) and (3.4) makes it possible to obtain the probability of activation P_j of any one of the mechanisms considered for the macroelement j, i.e. the probability of collapse of the macroelement. Note that the direction of the applied load is not explicitly taken into account when calculating the collapse probabilities.

Table 1 shows the types of macroelements and the relevant collapse mechanisms that have been considered in the presented application; typical examples of in-plane and out-of-plane collapse mechanisms are shown in Figs. 3, 4 and 5.

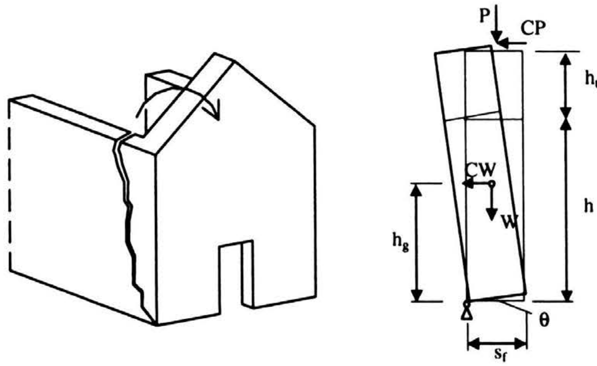

$$C_{1a,1} = \frac{(W+P)s_f - \frac{1}{2}\frac{(W+P)^2}{\sigma_k(\mu_b b)}}{Wh_g + P\left(h + \frac{h_t}{2}\right)}$$

σ_k: compressive strength of masonry
b: width of façade
$\mu_b b$: effective length of cylindrical hinge
h: height of the rectangular part of the façade
h_t: height of the triangle at the top of the façade
h_g: height of the centroid above the basis of the façade
s_f: thickness of the façade

FIGURE 3. Facade: collapse mechanism 1a (see Table 1); detachment from orthogonal walls and out-of-plane rotation due to the development of a horizontal cylindrical hinge at the basis of the facade.

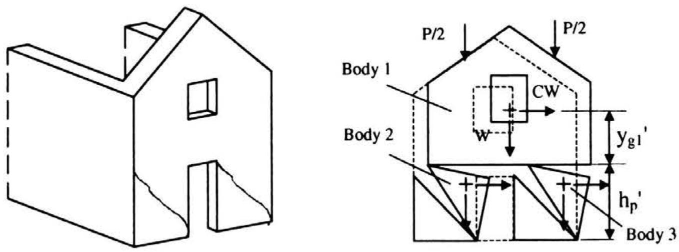

$$C_{3a,1} = \frac{W_1\delta_{yg1} + 2W_2\delta_{yg2} + P\delta_{yP}}{W_1\delta_{xg1} + 2W_2\delta_{xg2} + P\delta_{xP}}$$

W_1: weight of body 1
$W_2 = W_3$: weight of bodies 2 and 3
P: weight of the roof
δ_{xg1}, δ_{yg1}: horizontal and vertical displacement of body 1
δ_{xg2}, δ_{yg2}: horizontal and vertical displacement of bodies 2 and 3
δ_{xP}, δ_{yP}: horizontal and vertical displacement of the roof

FIGURE 4. Facade: collapse mechanism 3a (see Table 1); in-plane failure due to cracks with x trend.

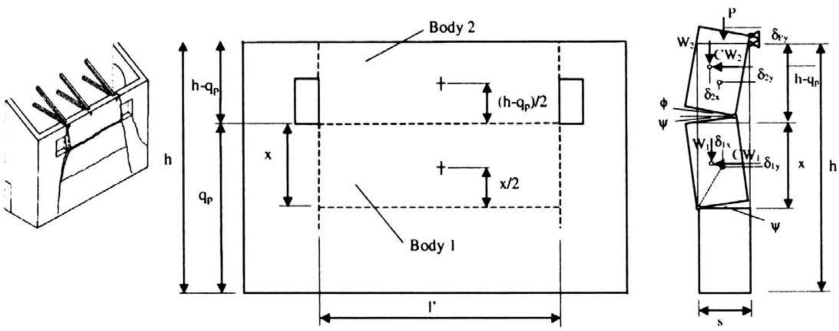

$$C = \frac{\left(\frac{W_1 s}{2} - \frac{2}{3}\frac{W_1^2}{\sigma_k l'}\right)\psi + \left(\frac{W_2 s}{2} - \frac{2}{3}\frac{W_2^2}{\sigma_k l'}\right)(\psi + \phi) + \left(W_1\delta_{1y} + W_2\delta_{2y} + P\delta_{Ny}\right)}{W_1\delta_{1x} + W_2\delta_{2x}}$$

σ_k: compressive strength of masonry
h: height of the lateral wall
q_p: height of the openings above the basis of the wall
s: thickness of the lateral wall
W_1: weight of body 1
W_2: weight of body 2
P: weight of the roof
δ_{1x}, δ_{1y}: horizontal and vertical displacement of body 1
δ_{2x}, δ_{2y}: horizontal and vertical displacement of body 2
δ_{Px}, δ_{Py}: horizontal and vertical displacement of the roof
x: distance between the openings and the cylindrical hinge
ψ: rotation angle of the bottom part of the wall
φ: rotation angle of the top of the wall

FIGURE 5. Nave lateral wall: collapse mechanism 4b (see Table 1); out-of-plane rotation of a wall restrained on the four sides.

Table 2 shows examples of logical combinations of mechanisms leading to the evaluation of the collapse probability P_j of each considered macroelement.

TABLE 2. Logical diagrams for evaluating the collapse probability P_j of the j-th macroelement (me stands for mutually exclusive, ind for independent mechanisms).

Macroelement	Collapse Probability
Facade (transept facade)	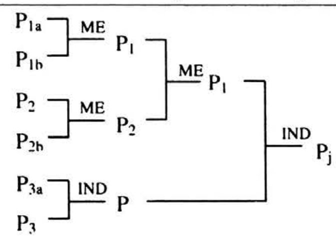
Nave (transept nave) (presbytery)	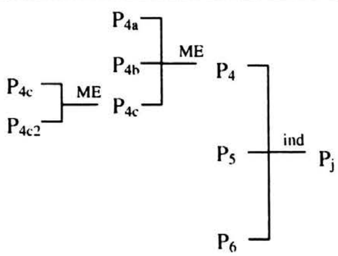
Triumphal arch	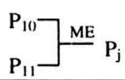
Apse (lateral chapels and annexes)	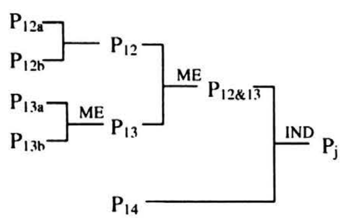

3.1.2. For the whole church: In most cases, the collapse of a building construction as a whole can be defined only conventionally. In fact collapse cannot be identified with the collapse of a single element, because each element may have a different role in the resistance of the whole.

Thus, the probability of collapse of the church would be underestimated if it were measured by the probability of collapse of just one macroelement; it is rather a function of the probabilities of collapse of the macroelements according to the functional logic of the whole system. Therefore, in order to assess the seismic vulnerability of the church, it is essential to consider both the different relevance of macroelements and the contribution of the vulnerability of each macroelement to the vulnerability of the whole.

The collapse condition of the whole must be defined according to the interaction between macroelements towards structural integrity, that is defined by a logical diagram.

Specifically:

(g) Macroelements are divided into *critical* macroelements, whose collapse involves destruction of the whole building, and *non critical* macroelements whose collapse does not necessarily imply complete destruction of the building. The whole church can thus be seen as a series system, composed of critical macroelements and subsystems, in turn made of non critical macroelements working in parallel.

(h) For each value of a_g, the collapse probability of each subsystem composed of macroelements working in parallel is evaluated by:

$$P_{f,\mathrm{par}} = \prod\nolimits_k P_k, \tag{3.5}$$

where P_k is the collapse probability of each branch k of the parallel subsystem.

(i) The collapse probability of the whole church is evaluated using the usual relation valid for series systems:

$$P_f = 1 - \prod\nolimits_m (1 - P_m), \tag{3.6}$$

where P_m includes the collapse probability P_j (3.4) of each critical macroelement and the collapse probability $P_{f,\mathrm{par}}$ (3.5) of each parallel subsystem.

3.2. Evaluation of the probability distribution of damage

The procedure illustrated in Sec. 3.1 can also be used to evaluate the *probability distribution of damages* (expressed in an appropriate damage scale), on the basis of the calculated probabilities of collapse for each macroelement and for the whole building.

This evaluation may support a statistical assessment of the distribution of damages to buildings formed by an arrangement of similar macroelements in a whole region hit by the earthquake.

3.2.1. For each macroelement: First, an appropriate *scale of damage* must be defined, enabling to describe different states of each macroelement, from no damage condition up to complete collapse. In the described application of the present procedure, a seven-level ($k = 0$ to 6) scale has been used; the seven damage levels k have been defined to correspond respectively to:

k=0: no evidence of damage;

k=1: first damages due to the inception of a mechanism, that can be detected only by an accurate examination;

k=2: significant damages and "readability" of the mechanism, activated but still at the initial stage of development;

k=3: clear and evident damages and "readability" of the mechanism, fully activated and at an intermediate stage of development;

k=4: macroscopically evident damages and full development of the mechanism, with some minor part of the macroelement at the limit of collapse because of significant overall movements;

k=5: as for k=4, but with significant parts of the macroelement at the limit of collapse and/or destruction and/or failures of other parts;

k=6: complete collapse.

As for the probability mass distribution of the damage to the macroelement, after relevant literature, it has been assumed that for any given value of a_{g} the binomial distribution can be adopted:

$$B(n,k,p) = \frac{n!}{k!(n-k)!}p^k(1-p)^{(n-k)}, \tag{3.7}$$

where:

- $B(n,k,p)$ is the probability of occurring a damage k in a scale of damage $0 - n$;
- k and n are positive integers;
- $k = 0, 1, \dots n$;
- $n = 6$ for the chosen scale;
- p is a parameter that defines the mean value of damage in a normalized damage scale ($0 \leqslant p \leqslant 1$).

The parameter p for the macroelement j is obtained by assuming that its collapse probability P_j, Eq. (3.4), is equal to the probability that the level of damage is equal to or larger than a *threshold level* n^*:

$$P_j = 1 - B_{\mathrm{cum}}(n,\, n*,\, p_j), \tag{3.8}$$

where $B_{\mathrm{cum}} = \mathrm{Prob}[k < n^*]$ is the cumulative distribution function (CDF) corresponding to the binomial distribution (3.7).

In the applications, the threshold level n^* has been taken equal to $n^* = 4$, since at this level the collapse mechanism of the macroelement is completely developed.

Once the p parameters that correspond to several different values of a_{g} have been evaluated for each macroelement, it is possible to calculate the probability of attaining each damage level in macroelements similar to the analysed one, even if they belong to different buildings.

3.2.2. For the whole church: As already noted in Sec. 3.1.2 with reference to collapse, the damage of the whole church can be defined only conventionally. In any case, a *scale of damage* must be defined, with the first level ($k = 0$) corresponding to no damage, and the last ($k = m$) to total ruin (overall collapse). However, for the whole church it is not possible to match each intermediate level of the scale with a well-defined physical condition, like in a macroelement the inception and successive evolution of the collapse mechanism; rather, the levels of the damage scale are made to correspond to qualitative judgements about the general condition of the building. In the numerical applications, it has been assumed $m = 10$ and its threshold value has been taken equal to $m^* = 7$.

As for each macroelement, it is assumed also for the whole church that a binomial distribution can be adopted for the probability of damage, for any given value of a_{g}:

$$B(m,\, k,\, q) \;=\; \frac{m!}{k!\,(m-k)!}\, q^k\,(1-q)^{(m-k)}, \tag{3.9}$$

where, in perfect analogy with Eq. (3.7)

- $B(m, k, q)$ is the probability to have a damage k in a scale of damage $0 - m$;
- k and m are positive integers;
- $k = 0, 1, \ldots m$;
- $m = 10$ for the chosen scale;
- q is a parameter that defines the mean value of damage in a normalized damage scale ($0 \leqslant q \leqslant 1$).

The value of the parameter q is obtained by assuming that the collapse probability of the whole church P_{f}, Eq. (3.6) is equal to the probability that the level of damage is equal to or larger than the value $m^* = 7$ (threshold level), at which level the condition of irreversible failure is considered to have been reached:

$$P_f = 1 - B_{\mathrm{cum}}(m,\, m^*,\, q). \tag{3.10}$$

Once the q parameters for the whole building corresponding to different values of a_g have been evaluated, it is possible to calculate the probability of finding each damage level in buildings similar (for typology and topological distribution of macroelements) to the building directly analyzed.

4. Example of application of the kinematic approach: *Santa Maria del Fossale*

As an example, the application is reported of the described procedure to the church of *Santa Maria del Fossale* in the town of Gemona, whose plan has been shown in Fig. 2. The following material parameters, typical of the churches in that area, have been used:

- weight density $= 18\,\mathrm{kN/m^3}$,
- compressive strength $= 2000\,\mathrm{kN/m^2}$,
- tensile strength $= 100\,\mathrm{kN/m^2}$,
- shear strength $= 150\,\mathrm{kN/m^2}$.

The other relevant data have been taken from [Doglioni *et al.* 1994].

The structural system is considered as the assemblage of the following macroelements (Fig. 2):

1 – facade,

2 – nave right wall,

3 – nave left wall,

4 – triumphal arch,

5 – apse.

It is also assumed that the collapse of any macroelement implies the "destruction" of the whole church: consequently; the macroelements are related in series in the logical diagram (Fig. 6).

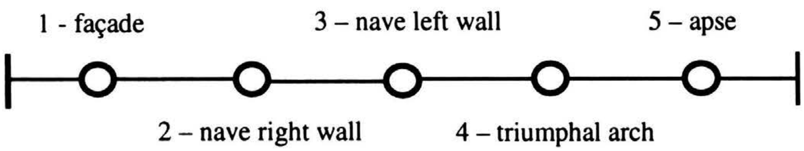

FIGURE 6. Logical diagram of the church of Santa Maria del Fossale, Gemona.

The nominal *mechanism seismic coefficients* C_{ij} of the macroelements have been calculated, as described in Sec. 3.1.1, by means of limit analysis, taking into account the collapse mechanisms of Table 1. Some examples of formulae yielding C_{ij} have been shown in Figs. 3, 4 and 5.

The values of the C_{ij}'s are reported in Table 3 as mean values, together with their estimated coefficients of variations (c.o.v.). Lacking a more precise evaluation, the c.o.v.s have been estimated in a very rough and empirical way, that is:

(i) the relevant random variables have been classified into four categories, according to their uncertainty (geometrical parameters; self weight and permanent actions; mechanical parameters, like compressive strength of masonry; mechanical parameters, like shear strength of masonry);

(ii) the weights 0.015, 0.075, 0.075, 0.100 have been respectively associated to each category;

(iii) finally, the c.o.v.s of the seismic coefficients have been obtained by multiplying each weight for the number of random variables of the corresponding category entering their definition and summing up.

In Table 3, also the probabilities P_{ij} of activation of the i-th mechanism for the j-th macroelement are shown for three values of a_g.

TABLE 3. Church of Santa Maria del Fossale: seismic coefficient C_{ij} (calculated mean values and estimated coefficients of variation) and probability P_{ij} of activation of mechanism i in macroelement j.

Mechanism (see Table 1)	Macroelement (see Fig. 2)	$E[C_{i,j}]$	c.o.v.	P_{ij} (a_g =0.16 g)	P_{ij} (a_g =0.28 g)	P_{ij} (a_g =0.40 g)
1a	1	0.146	0.375	0.601	0.993	1.000
1b	1	0.191	0.375	0.332	0.893	0.998
2a	1	0.845	0.390	0.019	0.043	0.089
2b	1	0.399	0.465	0.099	0.260	0.502
3a	1	1.122	0.325	0.004	0.010	0.024
3b	1	0.866	0.390	0.018	0.041	0.084
4a	2, 3	0.191	0.450	0.358	0.848	0.992
4b	2, 3	0.460	0.315	0.019	0.107	0.339
$4c_1$	2, 3	0.086	0.345	0.994	1.000	1.000
$4c_2$	2, 3	0.098	0.345	0.966	1.000	1.000
5	2, 3	1.602	0.305	0.002	0.003	0.007
6	2, 3	1.472	0.355	0.006	0.011	0.020
10	4	0.896	0.400	0.020	0.043	0.083
11	4	0.474	0.375	0.039	0.138	0.339
12a	5	0.218	0.390	0.248	0.768	0.984
13	5	0.286	0.405	0.138	0.479	0.837
14	5	2.141	0.265	0.000	0.001	0.001

TABLE 4. Church of Santa Maria del Fossale: evaluation of the weighting factors for collapse mechanisms number 4a, 4b, 4c of the macroelement "nave right wall" ($j = 2$), (a – connection between lateral walls and transversal elements (facade and triumphal arch); b – tie rods between the tops of the lateral walls).

Case	1	2	**3**	4
a	yes	yes	**no**	no
b	yes	no	**yes**	no
$w_{4a,2}$	0.20	0.6	**0.10**	0.10
$w_{4b,2}$	0.70	0.1	**0.80**	0.10
$w_{4c,2}$	0.10	0.3	**0.10**	0.10

In Table 4, an example is reported of the evaluation of the weighting factors w_{ij} carried out for a specific macroelement (the nave right wall, $j = 2$) and the collapse mechanisms 4a, 4b, 4c (cf. Table 1); four alternative sets of coefficient are shown, which depend on: a) a judgement on the degree of connection between the lateral wall and the orthogonal ones, and b) on the presence or the lacking of tie rods between the tops of the lateral walls.

TABLE 5. Church of Santa Maria del Fossale: weighting factors w_{ij}.

Mechanism i (see Table 1)	Macroelement j (see Fig. 2)	Weight factors w_{ij}
1a	1	0.80
1b	1	0.20
2a	1	0.20
2b	1	0.80
1	1	0.40
2	1	0.60
$4c_1$	2, 3	0.78
$4c_2$	2, 3	0.22
4a	2, 3	0.10
4b	2, 3	0.80
4c	2, 3	0.10
10	4	0.30
11	4	0.70
12a	5	0.20
13	5	0.80

The actual macroelement is in case 3 (poor connection with the orthogonal walls and presence of tie rods) and the corresponding set of w_{ij} has been used in the calculations.

The entire sets of weighting factors w_{ij} evaluated in this way for the church of *Santa Maria del Fossale* is reported in Table 5.

The probability of collapse P_j of each macroelement, calculated for three peak ground accelerations a_g as discussed in Sec. 3.1.1(e) and in accord with the logical diagrams in Table 2, are shown in Fig. 7 together with the corresponding probabilities of collapse of the whole church, calculated as in Sec. 3.1.2 with the logical diagram of Fig. 6.

Figure 8 shows the relations between collapse probabilities and earthquake intensity (*fragility functions*) calculated for each macroelement and for the whole church.

Finally, the parameters of the binomial distributions of damage, for each single macroelement and the whole church, are reported in Table 6.

TABLE 6. Church of Santa Maria del Fossale: values of parameter p, Eq. (3.7), and of parameter q, Eq. (3.9), of the probability mass distributions of damages of the macroelements and to the whole church, for the assumed threshold damage values (respectively $n^* = 4$ and $m^* = 7$) and three values of the horizontal load coefficient a_g/G.

	$a_g = 0.16\,g$	$a_g = 0.28\,g$	$a_g = 0.40\,g$
1 – facade	0.632	0.544	0.688
2, 3 – left and right nave walls	0.544	0.629	0.729
4 – triumphal arch between nave and presbytery	0.382	0.500	0.618
5 – apse	0.588	0.702	0.802
whole church	0.770	0.885	0.955

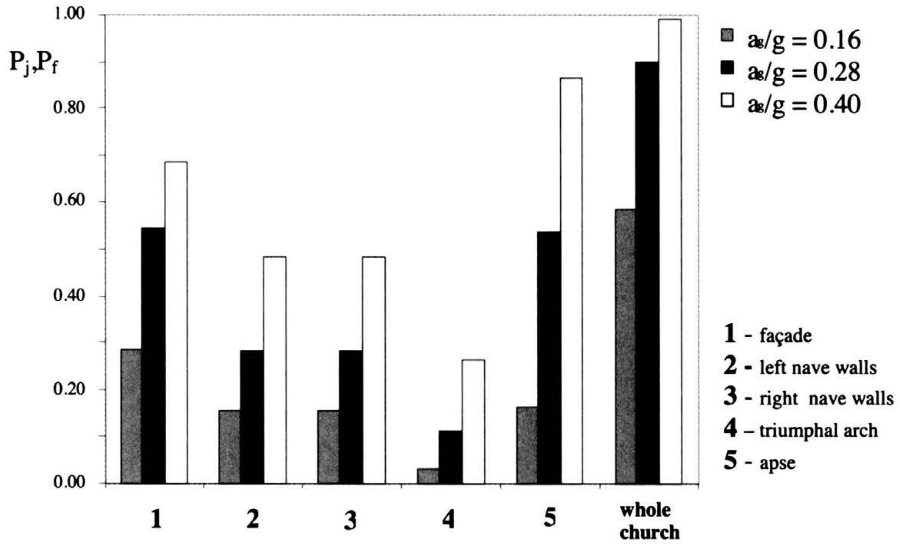

FIGURE 7. Church of Santa Maria del Fossale: collapse probabilities P_j of the macroelements, and collapse probability P_f of the whole church, evaluated for three values of the seismic coefficient a_g/g.

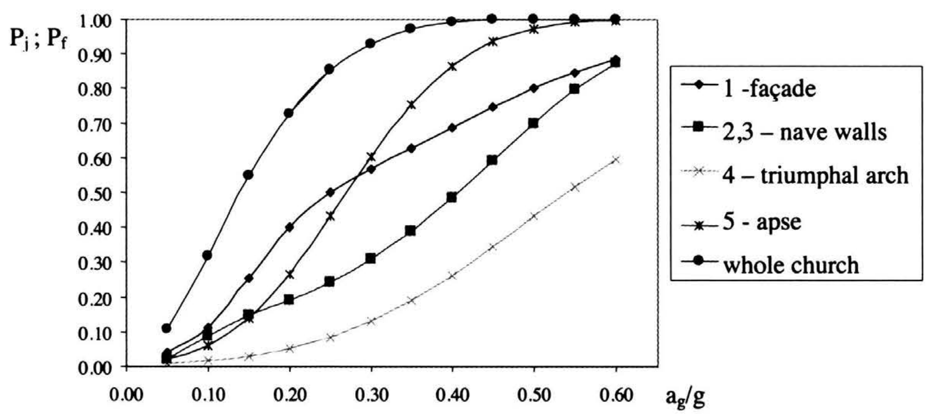

FIGURE 8. Church of Santa Maria del Fossale: fragility functions (collapse probability vs. seismic coefficient a_g/g) of the macroelements and of the whole church.

5. Bounding the probability of collapse by combining static and kinematic approaches. A case example: the church of *Santa Maria Maddalena*, in Flagogna

A more complete (i.e. kinematic and static) limit analysis has been developed for the church of *Santa Maria Maddalena* in Flagogna (Fig. 9).

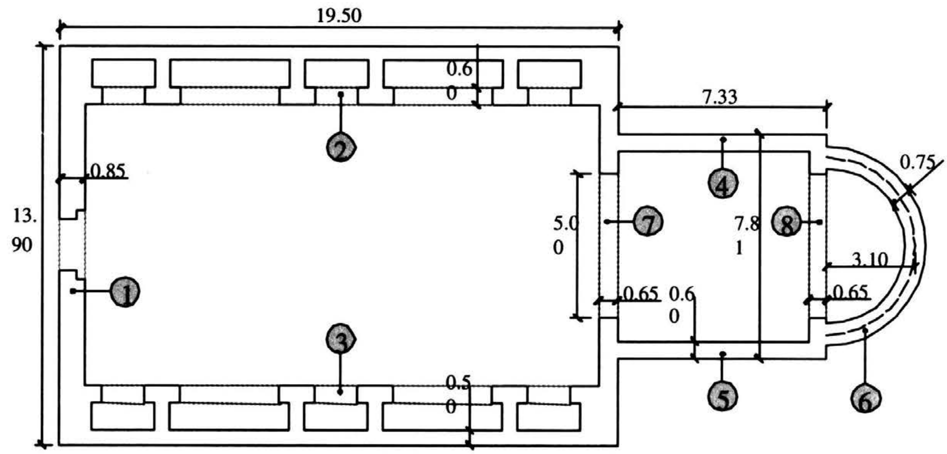

FIGURE 9. Church of Santa Maria Maddalena, in Flagogna (Friuli, Italy). Plan and considered macroelements: 1 – facade; 2 – nave left wall; 3 – nave right wall; 4 – presbytery left wall; 5 – presbytery right wall; 6 – apse; 7 – triumphal arch between nave and presbytery; 8 – triumphal arch between presbytery and apse.

Let us illustrate the analysis of this church by the static approach first.

5.1. Analysis according to the static theorem

In investigating the admissible stress fields, the resistance condition is checked in control sections, namely: the bottom section of the macroelement; all discontinuity sections (e.g. at the basis and just above openings in the walls, or where the wall thickness varies abruptly); the sections with concentrated loads. Stresses are assumed to be linearly distributed in these sections, possibly piecewise constant. It is assumed that the strength of masonry follows the Mohr-Coulomb criterion with tension cut-off (Fig. 10).

In the specifically developed computer program, it is possible to assume as random the following variables:

- the mass density of masonry;
- the shear resistance τ_0, the friction angle φ and the cut-off value σ_t that completely define the strength criterion (Fig. 10);

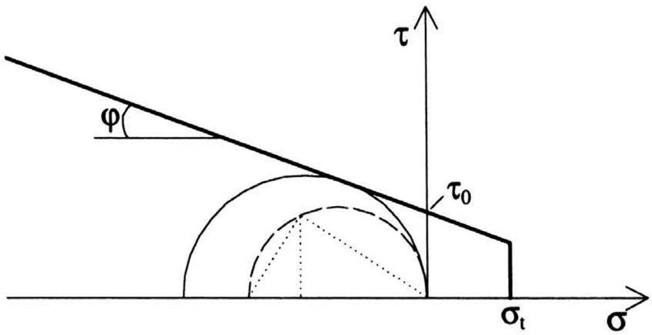

FIGURE 10. Mohr-Coulomb criterion with tension cut-off.

- the external vertical loads acting on each macroelement;
- some internal forces in the masonry structure modeling the connection between orthogonal walls or the restraint conditions along the border.

It is convenient to collect these variables into a vector $\mathbf{X}$ of random components X_q.

As anticipated in Sec. 2, in this example all random variables have been assumed to be described by discrete probability density (or "mass") functions [pmf] (uniform or binomial): thus, all possible combinations of values of the random variables, each characterized by a probability, form a finite set.

In order to reduce the number of possible combinations, it is important to select, for each macroelement, the most important random variables: this has been done by means of preliminary sensitivity analyses.

Thus, the following variables X_q have been considered random in numerical calculations:

- the shear resistance τ_0 of masonry;
- a concentrated force F, orthogonal to the considered element, that models the constraint effect of adjacent orthogonal elements.

The assumed probability mass functions of these two variables are shown in Figs. 11(a-c): two alternative distributions of F have been considered in relation to the efficiency (good or poor) of the constraint.

Also the direction θ of the horizontal load action has been taken as a random variable with a discrete probability distribution, and in particular a uniform distribution (Fig. 11(d)).

To carry out the calculations, first an arbitrary direction $\theta = i$ of the horizontal action and a combination $\mathbf{X}_j$ of the values of the X_q random variables (τ_0 and F in the developed example) are chosen. The problem becomes

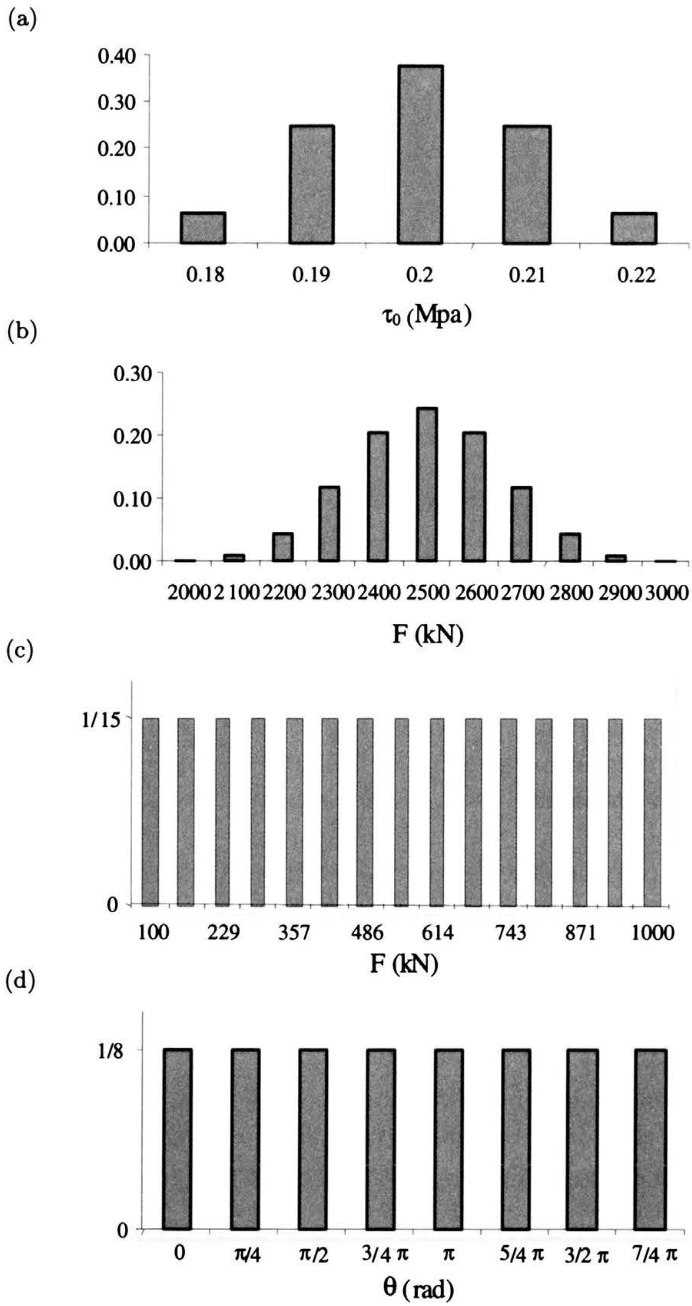

FIGURE 11. Probability mass functions of assumed random variables: (a) shear resistance τ_0; (b) efficient constraint force F; (c) poor constraint force F; (d) direction θ of the horizontal action.

deterministic, and the probability of not finding a statically admissible stress field under these conditions is by definition given by:

$$P\left[E_{\text{stat},ji}\right] = P\left[E_{\text{stat}} \mid \theta = i,\ x = X_j\right] = \begin{cases} 0 & \text{if } \alpha \leqslant \alpha_{\psi_{ji}}, \\ 1 & \text{if } \alpha > \alpha_{\psi_{ji}}, \end{cases} \tag{5.1}$$

where $\alpha_{\psi ji}$ is the value of the statically admissible load factor for the j-th combination of r.v.s and the i-th load direction. As already stated (Fig. 1 and Eq. (2.4)), the values of $\alpha_{\psi ji}$ for each direction i are calculated by interpolating linearly the values corresponding to two "principal" orthogonal directions (for walls and arches, in-plane and out-of-plane directions). Equation (5.1) is represented by a $0-1$ step function with discontinuity at $\alpha = \alpha_{\psi ji}$ (Fig. 12).

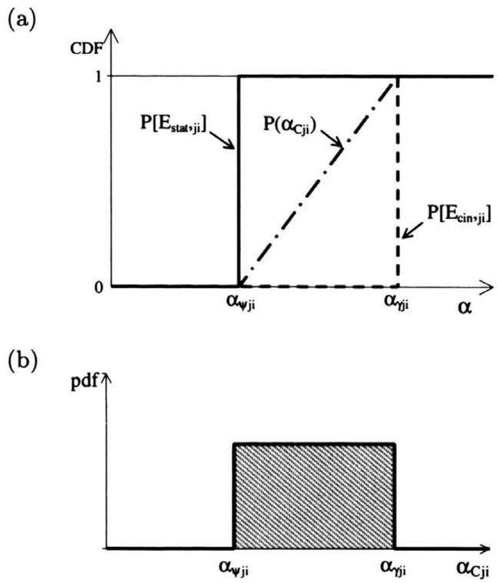

FIGURE 12. (a) Probability distribution functions of the statically admissible load factor $\alpha_{\Psi_{ji}}$, the kinematically sufficient load factor $\alpha_{\gamma_{ji}}$, and an approximation of the "true" value of the collapse load factor; (b) probability density function of the approximated $P(\alpha_{C_{ji}})$.

If, as assumed, each of the random variables X_q can take only a finite number of values X_{qj}, the number N of their possible combinations can be large, but – as already stated – is finite. Assuming moreover that the variables X_q are statistically independent of each other (as it seems reasonable for τ_0 and F), the probability of not finding a statically admissible stress field, for any given load direction $\theta = i$ becomes:

$$P\left[E_{\text{stat}}\,|\theta = i\right] = \sum_{j=1}^{N} P\left[E_{\text{stat}}\,|\theta = i,\ X = X_j\right] \cdot P\left[X = X_j\right]$$
$$= \sum_{j=1}^{N} P\left[E_{\text{stat}}\,|\theta = i,\ X = X_j\right] \cdot \prod_{q=1}^{Q} P\left[X_q = X_{qj}\right]. \quad (5.2)$$

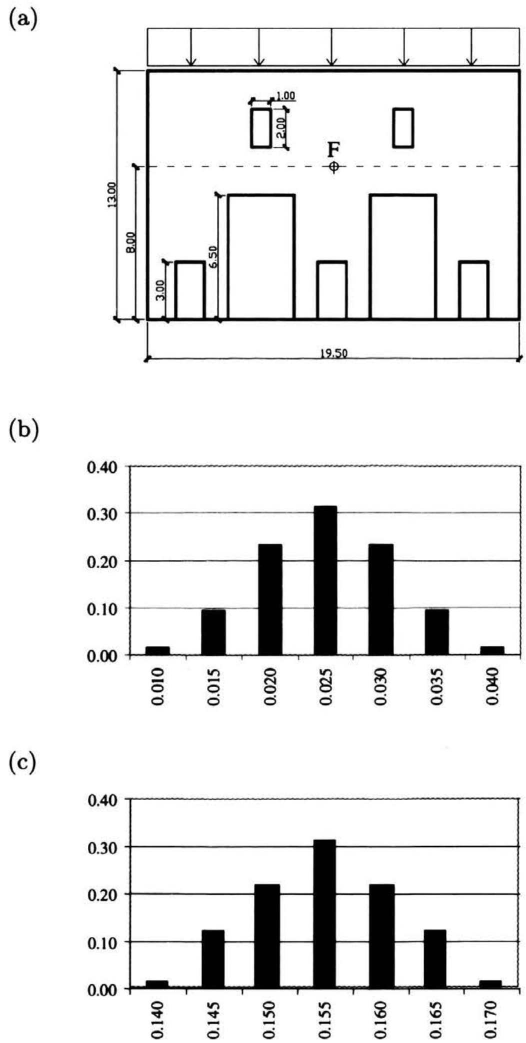

FIGURE 13. Nave wall: (a) geometry; probability mass functions of the largest admissible horizontal load acting in (b) out-of-plane-direction and (c) in-plane direction.

An example of the pmf's of the horizontal statically admissible load $\alpha_{\psi_i}\mathbf{W}$ calculated in this way for a specific macroelement (the nave walls – macroelement 2, 3) in the two "principal" load directions, is shown in Fig. 13.

Finally, the probability $P[E_{\text{stat}}]$ for an arbitrary load direction is obtained by summation of the probabilities (5.2) multiplied by the probability of each possible direction. Assuming n_{d} directions, each with the same probability $1/n_{\text{d}}$:

$$P\left[E_{\text{stat}}\right] = \sum_{i=1}^{n_{\text{d}}} P\left[E_{\text{stat}}\left|\theta = i\right.\right] \cdot P\left[\theta = i\right] = \frac{1}{n_{\text{d}}} \sum_{i=1}^{n_{\text{d}}} P\left[E_{\text{stat}}\left|\theta = i\right.\right]. \tag{5.3}$$

In the calculations, eight possible directions, each with a probability $1/n_{\text{d}} = 1/8$, have been assumed (Fig. 12d).

The CDF curves $P(\alpha_{\psi})$ plotted in Fig. 14 have been obtained taking account of the probabilities of each combination of r.v.s, as it will be illustrated later, by means of Fig. 15.

5.2. Kinematic analysis

In Secs. 3 and 4, the relevant collapse mechanisms of each macroelement were considered, and it was shown how nominal values of the *mechanism seismic coefficients* C_{ij} (i.e. the values of α that activates mechanism i in macroelement j) can be obtained from the nominal (i.e. mean) values of the quantities involved. Then, each C_{ij} was assumed to have a continuous probability distribution around its nominal value: the probability of activation of each mechanism under a load defined by the coefficient $\alpha = a_{\text{g}}/g$, coincides with the corresponding value of the cumulative distribution function (CDF) of C_{ij}, Eq. (3.1). Appropriate combination of the probabilities of activation of each mechanism allowed to obtain the probability of activation P_j of any one of the mechanisms considered for each macroelement j. If all possible collapse mechanisms had been considered in this process, P_j would be the actual collapse probability of macroelement j; otherwise, according to the kinematic theorem of probabilistic limit analysis, P_j yields only a lower bound. Examples of curves $P_j(\alpha)$ for each mechanism and corresponding CDFs $P_{\text{f}}(\alpha)$ for whole churches have been presented in Fig. 8.

As anticipated, a slightly different approach is at the basis of the $P(\alpha_{\gamma})$ curves drawn in Fig. 14.

Discrete rather than continuous probability distributions have been assumed for the structural characteristics, and a procedure similar to the one illustrated in Sec. 5.1 has been followed, adopting an analogous notation. First, for each macroelement, kinematically sufficient load factors $\alpha_{\gamma_{ji}}$

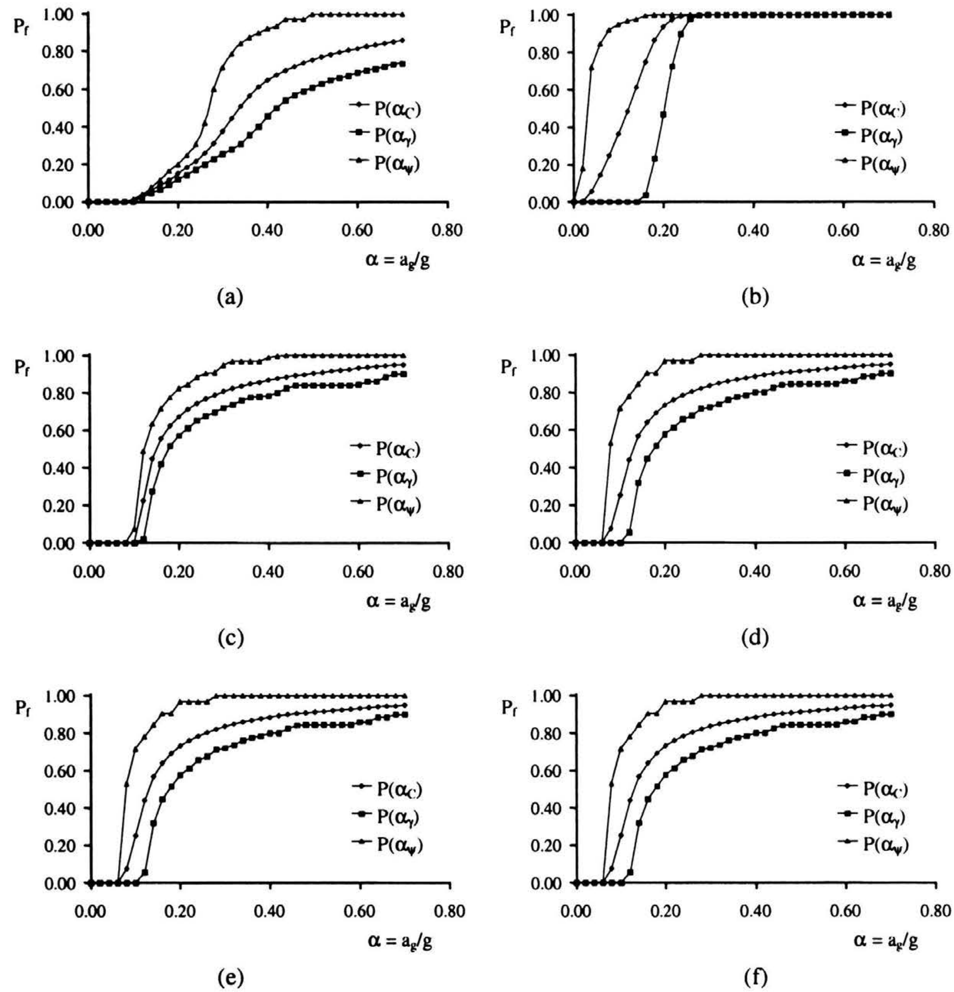

FIGURE 14. Probability bounds $P(\alpha_\Psi)$, $P(\alpha_\gamma)$; approximation to $P(\alpha_c)$: (a) macroelement 1 (facade); (b) macroelements 2, 3 (nave walls); (c) macroelements 4, 5 (presbytery walls); (d) macroelement 6 (apse); (e) macroelement 7 (arch between nave and presbytery); (f) macroelement 8 (arch between presbytery and apse).

have been determined for each combination $\mathbf{X}_j$ of the relevant random variables and direction i. In contrast to the static analysis presented in Sec. 5.1, the interaction diagram has been assumed rectangular, i.e. external to any convex diagram (cf. Fig. 1 and Eq. (2.5)). The corresponding probability $P[E_{\text{cin}}|\ \mathbf{X} = \mathbf{X}_j|\theta = i]$ is given by a $0 - 1$ step function with discontinuity at $\alpha = \alpha_{\gamma_{ji}}$ (Fig. 12).

Then, noting that the random variables X_q can each take only a finite number of values X_{qj}, the probability of finding a kinematically sufficient mechanism, for any assumed load direction $\theta = i$ becomes:

$$\begin{aligned} P[E_{\text{cin}} | \theta = i] &= \sum_{j=1}^{N} P[E_{\text{cin}} | \theta = i,\ X = X_j] \cdot P[X = X_j] \\ &= \sum_{j=1}^{N} P[E_{\text{cin}} | \theta = i,\ X = X_j] \cdot \prod_{q=1}^{Q} P[X_q = X_{qj}]. \end{aligned} \tag{5.4}$$

With a finite number of possible directions i of the load, the probability $P[E_{\text{cin}}]$ for an arbitrary load direction is obtained by summation of the probabilities (5.4) multiplied by the probability of each direction. Assuming that each direction has the same probability $1/n_{\text{d}}$, we get

$$P[E_{\text{cin}}] = \sum_{i=1}^{n_{\text{d}}} P[E_{\text{cin}} | \theta = i] \cdot P[\theta = i] = \frac{1}{n_{\text{d}}} \sum_{i=1}^{n_{\text{d}}} P[E_{\text{cin}} | \theta = i]. \tag{5.5}$$

The CDF's $P(\alpha_\gamma)$ plotted in Fig. 14 have then been obtained by considering many relevant mechanisms and all eight possible (and equally probable) directions of the seismic action.

5.3. An approximation of the probability of collapse

In previous Sections, CDF's of the statically admissible and kinematically sufficient load factors, respectively $P(\alpha_\psi)$ and $P(\alpha_\gamma)$, that – according to inequalities (2.8) – bound the CDF of the actual collapse loads factor $P(\alpha_{\text{C}})$, have been obtained for the macroelements indicated in Fig. 9. Note that the bounds on the probability of collapse obtained in this way (Fig. 14) are in most cases quite acceptable, especially in the range of significant values of the seismic intensity.

An approximation of the true curve $P(\alpha_{\text{C}})$ is also plotted in each of the graphs presented in Fig. 14. It has been calculated by assuming that, for each load direction θ_i and combination X_j of the other random variables, the value of the actual collapse load factor $\alpha_{C_{ij}}$ is a random variable uniformly distributed in the interval $[\alpha_{\psi_{ji}}, \alpha_{\gamma_{ji}}]$ (Fig. 13(b)); thus the corresponding CDF is the dash-dotted straight line.

The procedure followed to obtain the bounding curves $P(\alpha_{\psi_i})$, $P(\alpha_{\gamma_i})$ and the approximate curve is illustrated in Fig. 15, where three combinations of random variables are considered and three diagrams analogous to Fig. 12(a) are plotted on the left-hand side. Each diagram is multiplied by the probability P_j of the respective r.v. combination; as the three combinations of random variables are independent, it is straightforward to obtain by multiplication

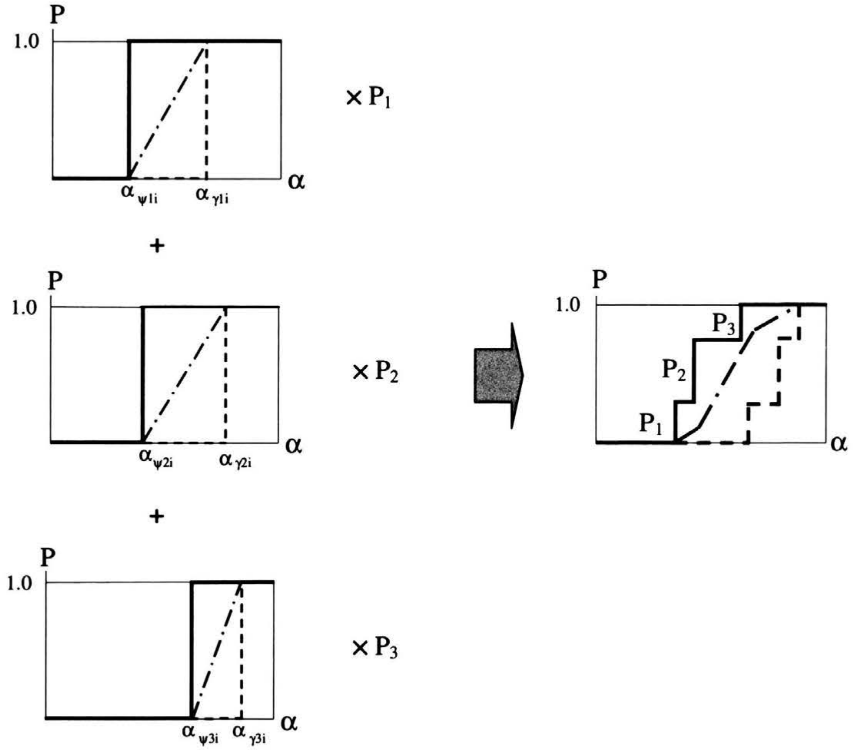

FIGURE 15. Construction of the bounding curves $P(\alpha_{\psi_i})$, $P(\alpha_{\gamma_i})$ and the approximate curve (dash-dotted).

and summation the probabilities of the collapse load factors $P(\alpha_{\psi_i})$, $P(\alpha_{\gamma_i})$, and the approximation.

The figure on the right is thus obtained. The three curves $P(\alpha_{\psi_i})$, and the approximation to $P(\alpha_{\gamma_i})$, $P(\alpha_{C_i})$ are obtained by increasing the number of combinations of r.v.'s (including also the random θ).

5.4. Limit analysis of the church

As already noted (Sec. 3.1.2), the collapse of a building as a whole can be defined only conventionally. In any case, in order to assess the seismic vulnerability of the church, it is essential to consider both the different relevance of macroelements and the contribution of the vulnerability of each macroelement to the vulnerability of the whole building system.

Figure 16 shows the logical diagram that has been assumed for the church of Santa Maria Maddalena: macroelements 1, 2 and 3 are considered *critical* macroelements, whose collapse implies the collapse of the whole church; col-

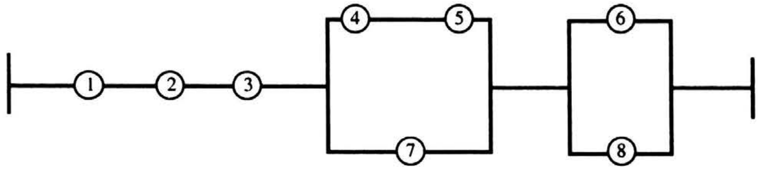

FIGURE 16. Logical diagram of the church of Santa Maria Maddalena, Flagogna.

lapse of the whole church is also implied by collapse of either macroelements 6 or 8, or by either collapse of macroelements 4 and 5, or of macroelement 7. The whole church is thus seen as a series system of five elements (the three critical macroelements and the two parallel subsystems).

Under the simplifying assumption of stochastic independence, for each seismic intensity the collapse probability of each parallel subsystem is given by Eq. (3.5), while the collapse probability of the whole church is given by Eq. (3.6), with P_m including the collapse probability P_j of each critical macroelement and the collapse probability $P_{f,\text{par}}$ of each parallel subsystem.

Bounds on the probability of collapse of the church have been evaluated by applying Eqs. (3.5) and (3.6) to the $P_k(\alpha_\psi)$ and $P_k(\alpha_\gamma)$ relative to each macroelement k: more specifically, for each direction $\theta = i$ of the horizontal load, the probabilities of collapse $P_k(\alpha_{\psi_i})$ and $P_k(\alpha_{\gamma_i})$ of each macroelement have been combined according to Eqs. (3.5) and (3.6). Then, bounds on the probability of collapse of the whole church for any load direction θ have been evaluated by applying Eqs. (5.3) and (5.5) respectively.

The values obtained are plotted in Fig. 17, together with the approximate curve $P(\alpha_C)$, obtained as described in Sec. 5.3. Also in this case, the bounds on the probability of collapse are quite acceptable.

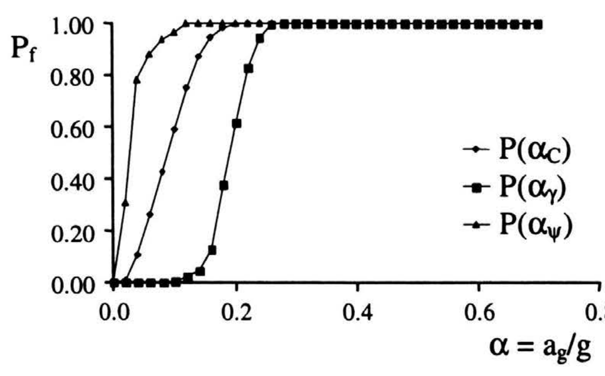

FIGURE 17. Santa Maria Maddalena, Flagogna: collapse of the whole church: probability bounds $P(\alpha_\Psi)$, $P(\alpha_\gamma)$; approximation to $P(\alpha_c)$.

6. Some final considerations

In this lecture, the concepts of reliability analysis have been applied to investigate the seismic vulnerability of a specific type of structural system, namely monumental buildings (and in particular, masonry churches).

In order to develop a mechanical model that can be applied without undue computational efforts, drastic simplifications have been introduced to describe seismic excitation and the corresponding structural responses. Namely:

- seismic loads have been represented by a set of static horizontal loads $\alpha\mathbf{W}$, where $\mathbf{W}$ stands for the weight of structural masses and other permanent vertical loads, and α is a coefficient that can be assimilated to the ratio a_g/g between the peak or effective horizontal ground acceleration and the acceleration of gravity g (the value α_C that corresponds to collapse of the building is by definition its *seismic coefficient*);
- the structural behaviour at collapse has been assumed to be well described by the macroelement approach.

These assumptions have made it possible to use the theorems of probabilistic limit analysis and bound the probability of collapse of the considered buildings from above and below.

Note also that the collapse of a church (but in general the same considerations might be repeated for any building construction) cannot be identified with the collapse of any single macroelement (in the more general case, of any component of the structural system); in order to assess the seismic vulnerability of the church, it is essential to consider both the different relevance of macroelements and the contribution of the vulnerability of each macroelement to the vulnerability of the whole.

Introducing discretized probability distributions for the relevant random properties involved in the problem, a concrete example of application has shown that, with a reasonable computational effort, the cumulative probability distributions $P(\alpha_C)$ of the seismic coefficients can be bounded between analogous curves $P(\alpha_\psi)$ and $P(\alpha_\gamma)$, relative respectively to statically admissible and kinematically sufficient seismic loads, $\alpha_\psi\mathbf{W}$ and $\alpha_\gamma\mathbf{W}$. The randomness of the direction of the horizontal action has also been taken into account.

Of course, the validity of the results obtained is limited by the introduced simplifying assumptions; therefore they should be considered only as approximations, that however can be very useful for a preliminary assessment of the seismic reliability of a large number of structures. The design of the retrofitting interventions for any specific example will of course require a more detailed structural analysis.

This lecture is based on two papers [1, 2], in which detailed lists of original references can be found.

References

1. G. AUGUSTI, M. CIAMPOLI, and P. GIOVENALE, Seismic vulnerability of monumental buildings, *Structural Safety*, Vol.23, No.3, pp.253-274, 2001.

2. G. AUGUSTI, M.CIAMPOLI, and S. ZANOBI, Bounds to the probability of collapse of Monumental Buildings, *Structural Safety*, Vol.24, Nos.2-4, pp.89-105, 2002.